Electronic Supplementary Material (ESI) for Dalton Transactions.

Crystal structure and planar defects in the layered honeycomb, delafossite-type materials $Ag_3LiIr_2O_6$ and $Ag_3LiRu_2O_6$

Sebastian Bette[*,a], Tomohiro Takayama[a,b], Viola Duppel[a], Agnieszka Poulain[c], Hidenori Takagi[a,b], Robert E. Dinnebier[a]

*S.Bette@fkf.mpg.de

[a] Max Planck Institut for Solid State Research, Heisenbergstraße 1, 70569 Stuttgart, Germany

[b] University of Stuttgart, Institute for functional Matter and Quantum Technologies, Pfaffenwaldring 57, 70569 Stuttgart, Germany

[c]European Synchrotron Radiation Facility (ESRF), 71 avenue des Martyrs, Grenoble, France

Additional Tables and Figures

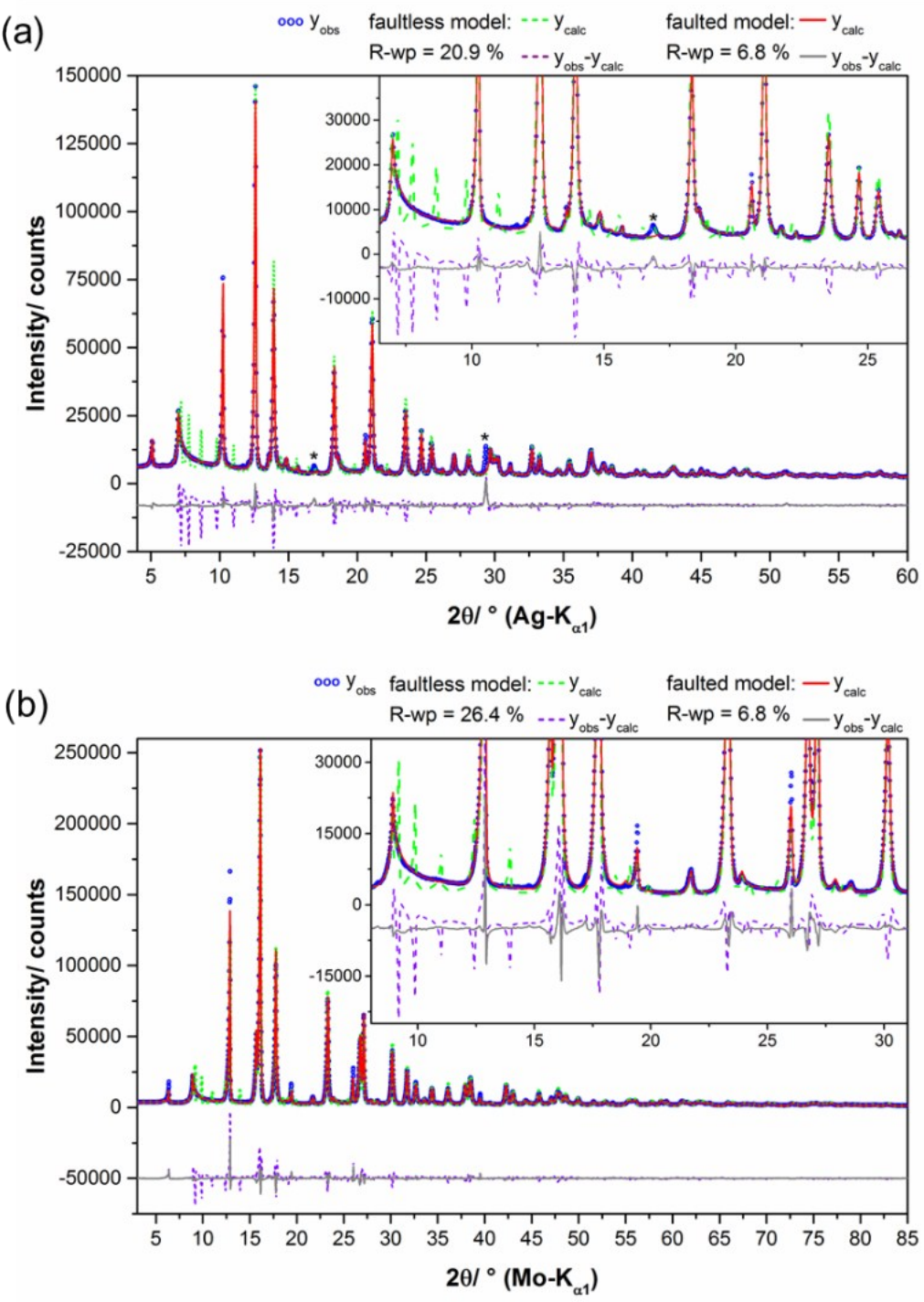

Figure S 1 Rietveld plots of the crystal structure refinements of $Ag_3LiIr_2O_6$ (a) and $Ag_3LiRu_2O_6$ (b) by using the ideal, faultless monoclinic structures (dashed lines) and by using supercell models with optimized faulting probabilities. Artificial peaks effects caused by the instrument are indicated by "*".

Table S 1. Rietveld Refinement data of $Ag_3LiIr_2O_6$ and $Ag_3LiRu_2O_6$ at ambient conditions.

sum formula	$Ag_3LiIr_2O_6$	$Ag_3LiRu_2O_6$
molar mass/ g·mol^{-1}	810.973	628.679
Wavelength / Å	0.5594	0.7093
R-p /% *	3.83	4.79
R-*w*p /% *	6.84	6.79
R-*F*² /% *	2.33	2.47
starting angle (° 2θ)	4	4
final angle (° 2θ)	60	85
step width (° 2θ)	0.001	0.001
time/scan (h)	15	15
no. of variables	39	39

* *R*-p, *R*-*w*p, and *R*-*F*² are given as defined in TOPAS (Bruker AXS) for the refinements using supercell sructures

Table S 2 Crystallographic data of isotypic layered honeycomb iridates and ruthenates at room temperature.

compound		**$Ag_3LiIr_2O_6$**	**$Ag_3LiRu_2O_6$**	**$H_3LiIr_2O_6$[1]**	
space group		*C*2/*m* (12)	*C*2/*m* (12)	*C*2/*m* (12)	
Z		2	2	2	
a **/Å**		5.287(1)	5.226(1)	5.349(1)	
b **/Å**		9.151(2)	9.036(1)	9.243(2)	
c **/Å**		6.503(1)	6.527(1)	4.873(1)	
α **/°**		90	90	90	
β **/°**		106.1(1)	105.7(1)	111.44(2)	
γ **/°**		90	90	90	
V **/Å³**		302.30(7)	296.66(6)	224.27(6)	
Atom	**Wyck.**	**site**	**S.O.F.**	**x**	**y**	**z**
			$Ag_3LiIr_2O_6$			
Ir(1)	4*g*	2	1	0	0.334(1)	0
Li(1)	2*a*	2/*m*	1	0	0	0
O(1)	4*i*	*m*	1	0.405(17)	0	0.189(8)
O(2)	8*j*	1	1	0.395(11)	0.332(1)	0.164(4)
Ag(1)	4*h*	2	1	1/2	0.332(1)	1/2
Ag(2)	2*d*	2/*m*	1	1/2	0	1/2
			$Ag_3LiRu_2O_6$			
Ru(1)	4*g*	2	1	0	0.334(1)	0
Li(1)	2*a*	2/*m*	1	0	0	0
O(1)	4*i*	*m*	1	0.390(14)	0	0.152(8)
O(2)	8*j*	1	1	0.398(9)	0.323(6)	0.164(4)
Ag(1)	4*h*	2	1	1/2	0.323(6)	1/2
Ag(2)	2*d*	2/*m*	1	1/2	0	1/2
			$H_3LiIr_2O_6$[1]			
Ir(1)	4*g*	2	1	0	0.335(3)	0
Li(1)	2*a*	2/*m*	1	0	0	0
O(1)	4*i*	*m*	1	0.404(8)	0.323(3)	0.229(5)
O(2)	8*j*	1	1	0.417(8)	0	0.220(9)

Table S 3 Selected bond distances of isotypic layered honeycomb iridates and ruthenates at room temperature

Bond	Distance/ Å		
	$Ag_3LiIr_2O_6$	$Ag_3LiRu_2O_6$	$H_3LiIr_2O_6$[1]
Ir(1)/Ru(1)-O(1)	2x 2.10(5)	2x 1.97(2)	2x 2.04(3)
Ir(1)/Ru(1)-O(2)	2x 2.07(5)	2x 2.07(4)	4x 2.01(3)
	2x 2.03(5)	2x 1.94(3)	
Li(1)-O(1)	2x 2.16(7)	2x 2.01(7)	4x 2.08(6)
Li(1)-O(2)	4x 2.04(3)	4x 2.07(3)	4x 2.15(3)
Ag(1)-O(2)	2x 2.09(3)	2x 2.11(3)	-
Ag(2)-O(1)	2x 1.94(5)	2x 2.17(5)	-

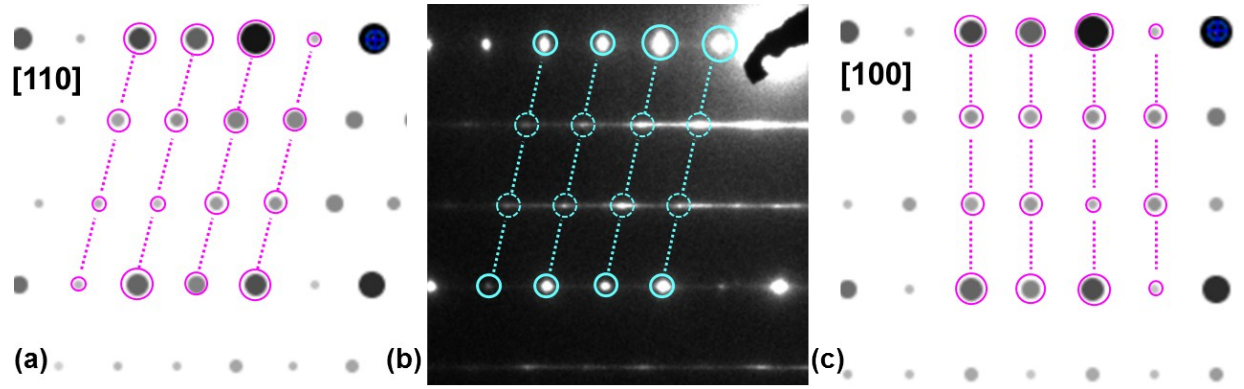

Figure S 2. Comparison of the measured (b) and the simulated (a,c) PED-patterns of $Ag_3LiRu_2O_6$. The positions of bright spots within the streaks is highlighted by light blue circles.

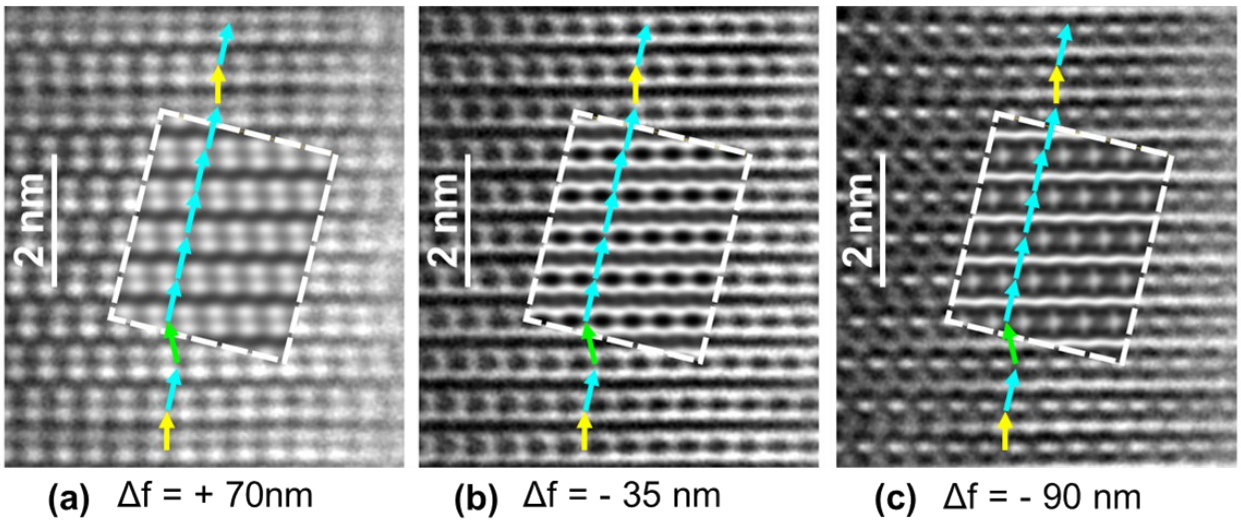

Figure S 3. HRTEM micrographs of $Ag_3LiRu_2O_6$ along zone axis [110] and simulated images (insets) with an assumed thickness of 5.22 nm.

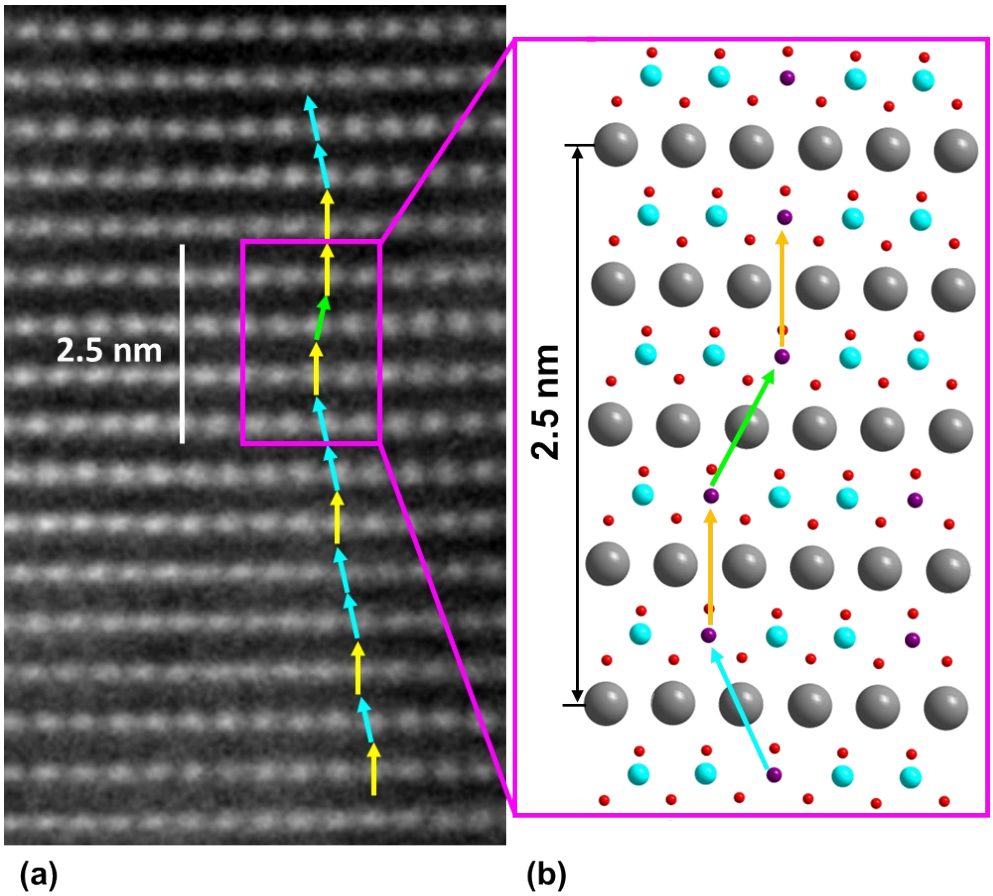

Figure S 4. HRTEM micrograph of Ag3LiIr2O6. The stacking order of the layers I s indicated by cyan, green and yellow arrows.

Table S 4. Selected commands in TOPAS syntax that were used to perform a grid search in the parameter space of the transition probabilities.

TOPAS-syntax	**Explanation**
num_runs 101	The input file is executed 101 times.
seed	Before execution of the input file the random number generator creates a new set of random numbers.
prm !px =(##Run_Number##)/100;	The run number is used as a running index, starting at 0, from one run to the next one the parameter P_x is increased by 0.01, which lead to $P_x = 1$ in the last run.
out "grid.txt" append Out(Get(r_wp),\t%11.5f) Out(pf, "\t%11.5f\n")	The R-wp value and the parameter value of P_x are stored in a separate ASCII file, as the INP-file is not modified and not OUT file is created when "num_runs" is used.

Table S 5. Overview on the pseudo-monoclinic constraints (indicated by bold, red font) that were applied to refine the layer constitution and the stacking vectors using a 200-layers supercell to approximate the microstructure of the sample.

site faultless structure	**site supercell structure**	***x***	***y***	***z***
Ru(1)	Ru(10)	0	**yru**	0
	Ru(11)	0	-**yru**	0
	Ru(12)	0.5	**yru**+0.5	0
	Ru(13)	0.5	-**yru**+0.5	0
Li(1)	Li(10)	0	0	0
	Li(11)	0.5	0.5	0
O(1)	O(10)	**xo1**	0	**zo1**/200
	O(11)	- **xo1**	0	**-zo1**/200
	O(12)	**xo1**+0.5	0.5	**zo1**/200
	O(13)	- **xo1**+0.5	0.5	**-zo1**/200
O(2)	O(20)	**xo2**	**yo2**	**zo2**/200
	O(21)	- **xo2**	**yo2**	**-zo2**/200
	O(22)	**xo2**	- **yo2**	**zo2**/200
	O(23)	- **xo2**	- **yo2**	**-zo2**/200
	O(24)	**xo2**+0.5	**yo2**+0.5	**zo2**/200
	O(25)	- **xo2**+0.5	**yo2**+0.5	**-zo2**/200
	O(26)	**xo2**+0.5	- **yo2**+0.5	**zo2**/200
	O(27)	- **xo2**+0.5	- **yo2**+0.5	**-zo2**/200
Ag(1)	Ag(10)	**xo2**	**yo2**	0.5/200
	Ag(11)	**xo2**	- **yo2**	0.5/200
	Ag(12)	**xo2**+0.5	**yo2**+0.5	0.5/200
	Ag(13)	**xo2**+0.5	- **yo2**+0.5	0.5/200
Ag(2)	Ag(20)	**xo1**	0	0.5/200
	Ag(21)	**xo1**+0.5	0.5	0.5/200

	stacking vectors		
vector	***x*-component**	***y*-component**	***z*-component**
S1	- **xo1**	0	1/200
S2-1	- **xo2**	- **yo2**	1/200
S2-2	(**xo1**+ **xo2**+0.5)-2	**yo2**-0.5	1/200
S2-3	(**xo1**+ **xo2**+0.5)-2	-**yo2**+0.5	1/200
S2-4	- **xo2**	**yo2**	1/200

References

1. S. Bette, T. Takayama, K. Kitagawa, R. Takano, H. Takagi and R. E. Dinnebier, *Dalton Trans.*, 2017, **46**, 15216-15227.